

Technique for Fast Detection of Short Circuit Current in PV Distributed Generator

RAJIV K. VARMA¹ (Senior Member, IEEE), SHAH ARIFUR RAHMAN¹ (Member, IEEE),
VISHWAJITSINH ATODARIA¹ (Student Member, IEEE), SIBIN MOHAN¹ (Member, IEEE),
AND TIM VANDERHEIDE²

¹Department of Electrical and Computer Engineering, University of Western Ontario, London, ON N6A 5B9, Canada

²Bluewater Power Distribution Corporation, Sarnia, ON N7T 7L6, Canada

CORRESPONDING AUTHOR: R. K. VARMA (rkvarma@uwo.ca)

This work was supported in part by the Ontario Centres of Excellence Grant CR-SG30-11182-11 including funding from Bluewater Power Distribution Corporation, Sarnia, and Hydro One Networks Inc., and in part by the NSERC.

ABSTRACT This paper proposes a new fast technique, in which the slope of a photovoltaic (PV) inverter current is utilized to predict if the current is expected to exceed its rated value due to any grid faults. Two applications of this technique are demonstrated. In jurisdictions where grid codes require distributed generators (DGs) to disconnect after a fault occurrence, such as in Ontario, Canada, this technique is utilized to rapidly disconnect the PV solar system even before the inverter short circuit current actually exceeds the rated current of the inverter, thereby obviating the problem of any adverse short circuit current contribution into the grid. However, in regions where grid codes require DGs to stay connected and provide grid support, such as low-voltage ride through, this technique can be used to rapidly and autonomously transform the PV solar farm into a dynamic reactive power compensator STATCOM (termed PV-STATCOM) for providing voltage support function. In this paper, the PV-STATCOM is used to stabilize a critical induction motor load in the vicinity of the solar farm, which would have otherwise become unstable due to the grid fault. PSCAD-based simulation studies are performed on a realistic distribution network to demonstrate the effectiveness of this technique.

INDEX TERMS Distributed generator (DG), flexible AC transmission system (FACTS), inverter, photovoltaic (PV) systems, protection, PV-STATCOM, short circuit current, STATCOM.

I. INTRODUCTION

In electric power systems, integration of more Distributed Generators (DGs) in the network increases the short circuit level due to the short circuit current contribution of the DGs during faults [1]–[4]. Compared to the synchronous and induction machine based generators the inverter based generators, such as Photovoltaic (PV) solar systems, contribute lower fault current to the network due to the characteristics of PV panels and inverter operation [2]. The short circuit current contribution from a PV system inverter is typically in the range of 1.2 times rated current for the large size inverter (1MW), 1.5 times (500kW) for medium size inverter and between 2 - 3 times for smaller inverters [5], [6]. Although, each PV solar farm may contribute short circuit currents as above, the total amount of fault current contribution may become unacceptably large for a feeder which has several PV systems connected [7], [8]. It is apprehended that

short circuit current contributions from multiple solar systems in the distribution feeders may add up to levels that could be damaging to the circuit breakers. Hence circuit breakers will need to be upgraded and substations will need to be modified at significant cost to the utility. This has resulted in the denial of about 45% applications for solar farm connections in Ontario, Canada, during 2011-13. Consequently a major effort was launched by CanSIA, the national trade association representing the solar energy industry in Canada, to investigate the true impact of short circuit currents from PV inverters, and their mitigation measures [5]. The objective was to prevent the loss of opportunity to integrate more PV based renewable generation in the Ontario distribution systems.

It is important to note that in Ontario, and in some other jurisdictions in Canada, it is required to disconnect the PV solar farms or any other DGs upon detection of fault on

the system [9]–[11]. However, in several jurisdictions such as Europe [12], [13] and recently in California [14], grid codes require the DG inverters to stay connected and provide Low Voltage Ride Through (LVRT) capability during fault scenarios. It is therefore important to detect the faults rapidly, and either disconnect the DGs from the network or provide grid support functions e.g. LVRT, as quickly as possible, depending upon the prevalent grid code requirements.

As a first step, adequate modeling of PV solar plants for predicting their short circuit contributions during network faults, is essential [2], [14], [15]. The traditional relay technologies mainly use overvoltage, undervoltage and overcurrent signals to detect the faults, and subsequently operate protective breakers [4], [16]. Continuous Wavelet Transform (CWT) has been used to process voltage and current transients for calculating the change in supply impedance. The occurrence of a grid fault can be identified within half a supply cycle and decision can be made if the fault requires a distributed generation unit to be disconnected [17]. A four-stage fault protection scheme against short-circuit fault for inverter based DGs is proposed in [18]. The inverter is initially controlled as a voltage source, which changes to the current controlled mode upon detection of the fault, thereby limiting the inverter output current. A lab validated pilot protection system based on time-synchronized measurements of instantaneous currents is proposed in [19], that is capable of tripping the fault in less than half a cycle.

Electronically triggered fault current limiters (FCL) have been used effectively to limit short-circuit currents [20]–[22]. Two types of FCLs are typically utilized. An un-interrupting FCL reduces the fault current magnitude to an acceptable level, which is about three to five times the maximum normal state current, which can be safely interrupted by the existing circuit breaker. An interrupting FCL can also act as a circuit breaker and interrupt the fault current. FCLs thus permit extending the service life of existing equipment while increasing the overall reliability of power systems due to their fast (almost instantaneous) operation. A concept of rate of change of current has been proposed as a minimum fault-current change limit to prevent nuisance current-limiter operation [23]. The current slope signal di/dt is utilized to detect a grid fault and rapidly operate a Fault Current Limiter in less than half a cycle [24].

So far, the above fast fault detection techniques have been used for protection of network and DGs; and for unsymmetrical fault detection in fault current limiters (FCL). However these techniques have not been used to prevent any short circuit current contribution in excess of the rated or utility-acceptable current output of PV solar inverters.

This paper presents a new fast short circuit current detection technique based on the rate of rise of current together with the current magnitude in a PV solar system based DG, deriving its concepts from the patent [25]. The short circuit current is detected very rapidly and any of the following two control operations can be initiated, per the applicable grid code in that region:

i) *Disconnect* the PV inverter before the current exceeds the rated output current of the inverter. This rapid disconnection of DG prevents the fault current to rise beyond the utility permissible limits. Implementation of such a strategy potentially alleviates the problem of short circuit currents from PV solar systems which led to the delay or denial of their connectivity in regions such as in Ontario. It is emphasized that the objective of the proposed technique is not to detect the occurrence of any fault in the network but only to identify such fault conditions during which the inverter short circuit current is likely to exceed its rated magnitude. The intent is to disconnect the inverter as rapidly as possible, as soon it is predicted that the short circuit current will reach limits considered unacceptable by the interconnecting utility.

ii) *Transform* the PV inverter into a dynamic reactive power compensator STATCOM and provide grid support functions.

A new concept of utilizing PV solar farms as STATCOM (PV-STATCOM) both during nighttime and daytime for different grid support functions was introduced in [26]–[28]. These functions include dynamic voltage support to increase the connectivity of neighbouring wind farms, enhance power transmission capacity through power oscillation damping, etc. The short circuit current detection technique proposed in this paper can be utilized to shut down the real power generating function of the PV solar farm very rapidly in the event of a fault, and autonomously transform the PV solar farm into a STATCOM (PV-STATCOM) with full inverter capacity. This smart inverter control concepts is based in part on the pending patent [29].

In this paper a case study is presented when a fault in the network causes a critical inductor motor load to get destabilized. Shutdown of these critical IM loads, even for a short duration of few minutes, can result in significant economic loss to the industrial facility using these IMs [30], [31], as the entire batch of materials (e.g. petrochemicals, automotive parts, chemicals, medicinal products) being transported/served by these motors may get damaged. The proposed technique does not disconnect the PV inverter. Instead it transforms autonomously and rapidly the PV solar inverter into a STATCOM and helps stabilize this critical induction motor load. An initial study on non-autonomous stabilization of induction motors using the concepts of the PV-STATCOM technology was discussed in [32].

In Section II, the study system model is described with the proposed controller. Section III presents case studies for symmetrical fault, asymmetrical fault and faults at different locations. Application of the proposed method for stabilizing a critical induction motor load is presented in Section IV. Discussions on the results are presented in Section V. Finally, Section VI concludes the research outcomes.

II. SYSTEM MODEL

The study system is comprised of a typical realistic distribution network with a PV solar farm [33] as shown in Fig. 1.

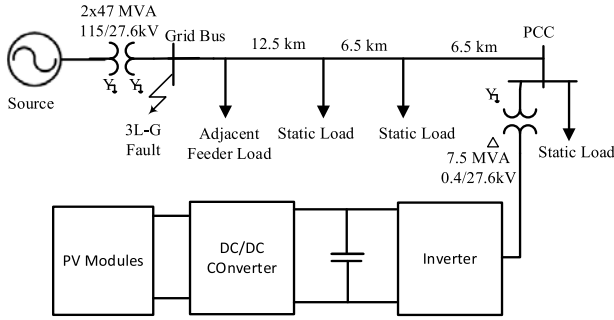


FIGURE 1. One line diagram of the study system.

A. SYSTEM DESCRIPTION

The study system consists of a 25 km long 27.6 kV feeder connecting the transmission network through a substation having two 47 MVA transformers [33]. The equivalent source impedance is combined with the transformer impedance in the system model. The overhead lines [34] and entire network is modeled in PSCAD/EMTDC software.

A total distributed load of 15 MVA is modeled as three groups of fixed impedance three phase static loads connected to the feeder and a large load at the end of the feeder. The adjacent feeder load of 60MW at 0.9 pf. is modeled as a single aggregated P-Q load connected at the beginning of the feeder. A 7.5MW PV solar farm is connected near the end of the feeder.

B. PV SYSTEM MODEL

Fig. 2 presents the detailed PV system model. The PV module in Fig. 2(a), boost converter and inverter in Fig. 2(b), AC filter in Fig. 2(c), Maximum Power Point Tracking (MPPT) module in Fig. 2(d) and the inverter controller in Fig. 2(e) constitute the conventional PV solar farm system.

The PV module is modeled as DC voltage controlled DC current source [35]. The boost converter and inverter along with its controller is used to transfer all the available power to the AC grid by regulating the DC voltage across the DC link capacitor with the use of DC link reference obtained from MPPT module. The boost converter [36] performs the MPPT and inverter regulates DC link voltage. The inverter maintains unity power factor operation by regulating reactive power output to zero.

The proposed fault detection module is shown in Fig. 2(f), and the internal circuit diagram of it is described in Fig 3. This module measures the instantaneous inverter output current and inverter terminal voltage. The measured instantaneous inverter output currents (I_{0_a} , I_{0_b} , I_{0_c}), are passed through a low pass filter to reject all the higher order harmonics or transients due to solar inverter injection, feeder capacitor switching or transformer energization [23], [24]. Subsequently the current signals are passed through two parallel paths in each channel; one path is through a slope detector (d/dt) and the other path is through a magnitude detector $|I|$. The slope detector is comprised of a comparator which compares the derivative of PCC current to determine the slope and compares with a reference slope $(d/dt)_{max}$.

For an inverter current $i = I_m \sin \omega t$, the reference slope or threshold limit can be determined approximately with the magnitude of (d/dt) of rated current as shown in the following expression [20]:

$$|di/dt| \approx k \omega I_m \quad (1)$$

where, I_m is the peak magnitude of instantaneous inverter current, k is an arbitrarily selected tolerance constant (typically chosen to be 1.0 - 1.06) based on the maximum inverter current injection considered acceptable by the utility during normal operating conditions, and ω is the fundamental angular frequency.

The magnitude detector is comprised of a comparator which compares the magnitude of PCC current with respect to a reference value $|I|_{max}$ which is the peak magnitude of instantaneous rated current.

It is understood that during large load switching near inverter terminal or during reclosure operation the rate of change of inverter current can cause a false triggering operation. In order to eliminate an unnecessary tripping of the inverters, the rate of change of voltage at inverter terminal is monitored. During a fault, the rate of change of voltage is higher compared to that during a large-load switching. Different faults and load switching studies are performed on the system to determine a threshold value for rate of change in voltage detector that can discriminate between a fault and load switching.

The trigger signal provided by the inverter current slope detector is enabled only if the rate of change in inverter bus voltage exceeds the predefined limit. The output of the slope detector is passed through an AND gate with the output of "rate of change in voltage" detector. Then this signal and output of magnitude detector is passed through the OR gate. Therefore, the output of these detectors goes high only if either of monitored values, (d/dt) or $|I|$ exceeds their corresponding reference values, $(d/dt)_{max}$ or $|I|_{max}$. The trigger signal is then passed to the flip-flop to hold the trigger signal once it goes high. The time delay in the clock signal of this S-R flip flop plays an important role to prevent the generation of any undesired trigger signal. Finally, the output of all triggering signals from all other channels are passed through a digital 'OR' gate to ensure that the output triggering signal 'PVIso' becomes high if a fault is detected in any of the phase current signals.

The PVIso signal can be used for different functions as required by the prevalent grid code, as described in the Introduction. Certain grid codes require fast isolation of PV inverter system during fault as in Ontario, Canada. For fast isolation of the inverter, the PVIso signal immediately stops the gating signals to IGBT through the ANDing operation with the inverter gating signals generated from the inverter and boost converter controller as demonstrated in Fig. 2. The PVIso signal is used to isolate the PV panel from the grid by using fast solid state switch as shown in Fig 2(g). As a result, the PV solar inverter stops the power transfer from the PV modules to the grid within few hundred micro-seconds

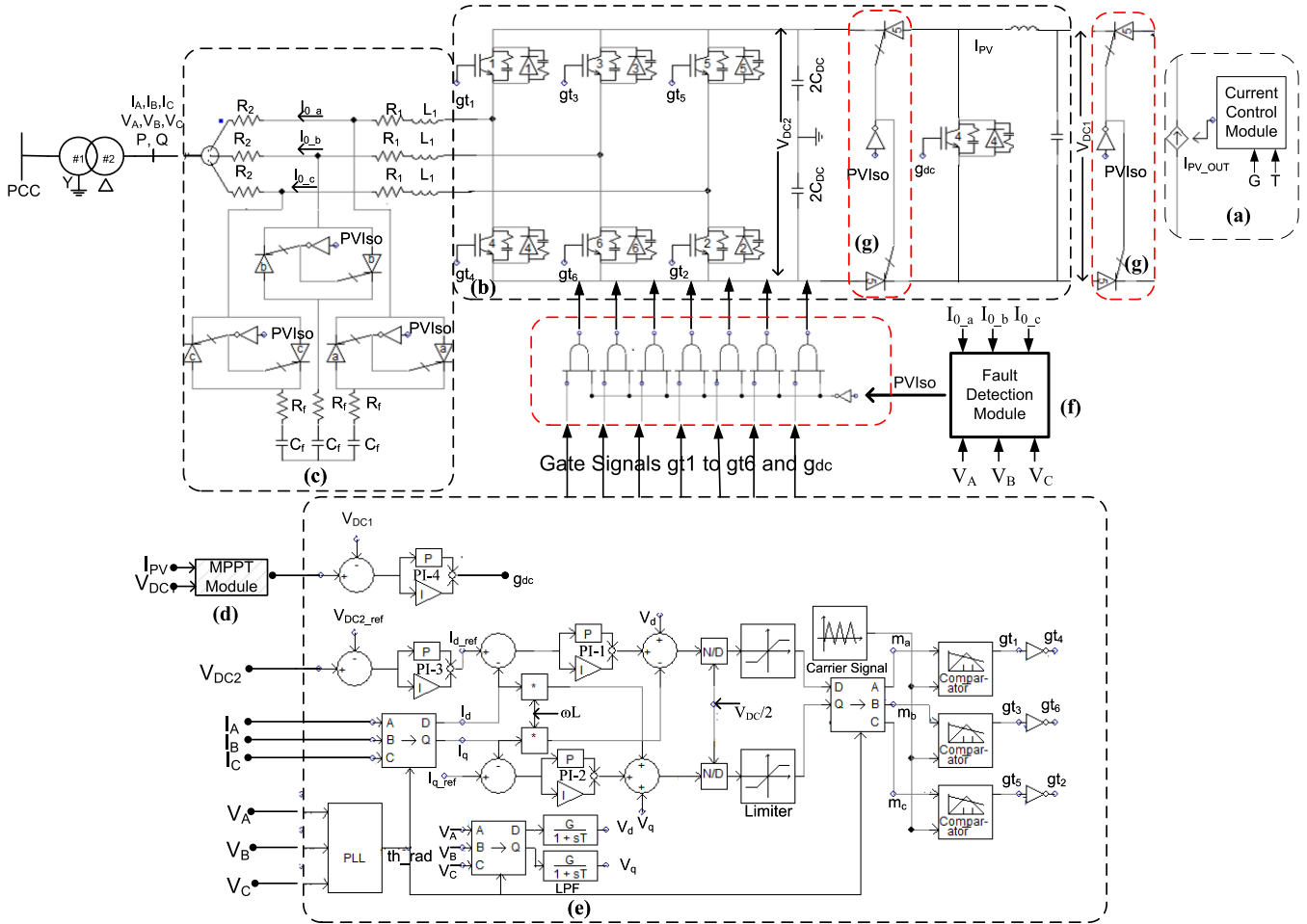


FIGURE 2. Detailed PV system inverter and conventional controller with incorporated fault detection module. (a) Model of PV solar panels. (b) Voltage source inverter. (c) LCL filter. (d) MPPT module. (e) Inverter control system. (f) Fault detection module. (g) Isolation of PV panels.

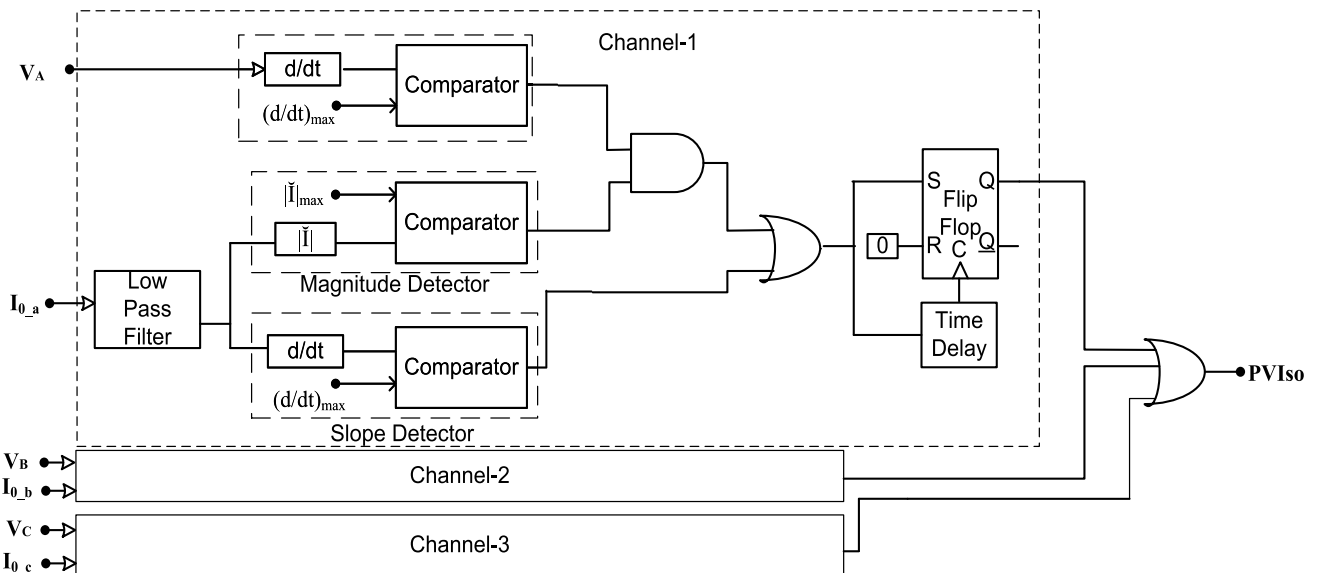


FIGURE 3. Fault detection module.

upon detection of any symmetrical or unsymmetrical fault in the grid. In addition, this triggering signal 'PVIso' is used

to isolate the AC filter capacitor by switching off the back to back connected gate turn off (GTO) thyristor or IGBT as

demonstrated in Fig. 2(c) to prevent high ringing currents between filter capacitance, C and inductance, L . This ringing phenomenon can also be suppressed by introducing sufficient damping resistor in the filter.

Certain other grid codes require Low Voltage Ride Through (LVRT) and grid support during fault. In this case, the PVIso signal can be used for enabling a faster LVRT or transformation of the PV inverter into a STATCOM (PV-STATCOM) for grid support.

The application of PVIso signal for fast transformation into a PV-STATCOM during fault and providing voltage support to stabilize a critical induction motor load, is described in Sections III and IV, respectively.

III. CASE STUDIES

Case studies are performed on the 7.5 MW PV solar system model as shown in Fig. 1 by applying different types of faults at PCC with proposed fault current controller enabled. The base value of a PV inverter current at PCC is 0.25 kA. The maximum rated value of PV inverter output current is 26.6 kA. As per (1), the reference value for rate limiter is 10023 [1/s] for $k = 1$. The low pass (transfer function) filter ($H = \frac{G}{1+s\tau}$) gives a delay time of 0.1 ms (with a setting of Gain (G) = 1 and Time constant (τ) = 0.0001 second, where phase delay angle = $\tan^{-1}(\omega RC) = 2.16^\circ = 0.0001$ second). $Triga$, $Trigb$, and $Trigc$ are the outputs of slope detector from the proposed controller for phase A, B and C, respectively. Similarly, $Magnitude Trigger$ is the resultant output of magnitude detector for all the three phases. PVIso is the triggering signal provided by the fault current controller. These conventions hold true for all PSCAD studies. The simulation results obtained from PSCAD are described below.

A. SYMMETRICAL FAULT

Fig. 4(a) demonstrates that the magnitude of inverter output current at PCC during line-to-line-to-line-to-ground (LLLG) fault at $t = 2$ second increases from 1 p.u. to 1.45 p.u. It is noticed from Fig. 4(b) that ' $Trigc$ ' signal becomes high within 0.3 ms from the initiation of fault in the grid, as slope of phase C (di/dt) has violated its permissible limit. Subsequently, $Trigb$ and other triggering signals also get high. However, the notable feature of the fault current controller is that only one triggering signal is needed to disconnect the PV inverter from the grid. Fig. 4(c) portrays the inverter current with the proposed fault detector module activated. The inverter shuts down and the inverter output current at PCC goes to zero in 0.8 ms. In addition, inverter current does not exceed its maximum rated value. Therefore, power system network does not see any short circuit current contribution from PV inverter.

B. ASYMMETRICAL FAULT

Fig. 5(a) depicts the inverter current after the occurrence of a single line-to-ground (SLG) fault at $t = 2$ second. The magnitude of inverter output current at PCC rises to 1.3 p.u.

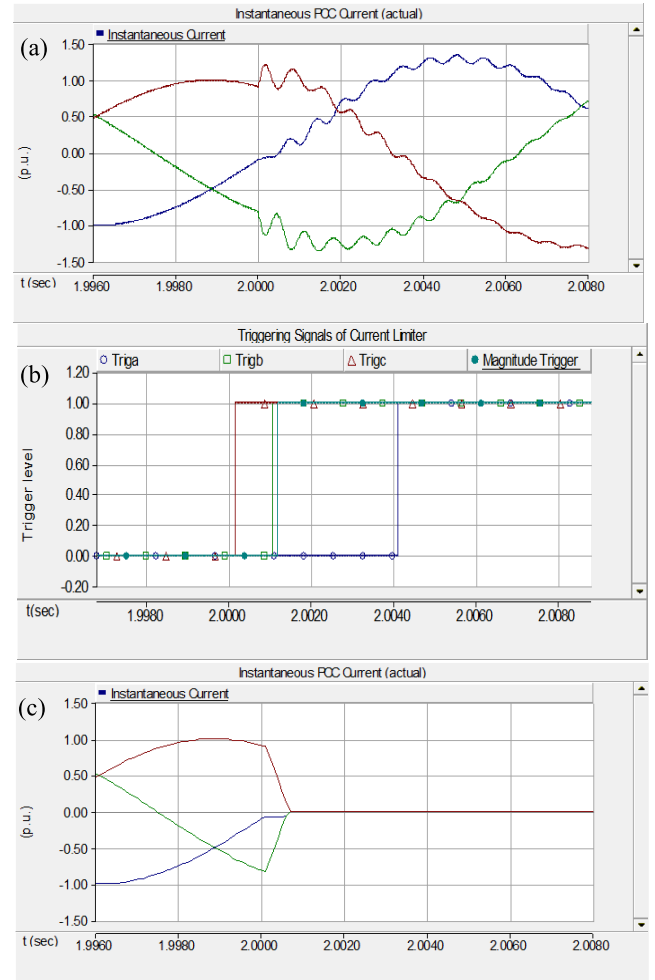


FIGURE 4. (a) Inverter fault current at PCC during LLLG fault at $t = 2$ seconds. (b) Triggering signals. (c) Inverter fault current with proposed fault controller.

It is observed from Fig. 5(b) that ' $Trigb$ ' signal becomes high after 1.1 ms from the initiation of fault, as slope of phase B current ($\frac{di}{dt}$) has exceeded its maximum allowable limit. As soon as the ' $Trigb$ ' signal becomes high, inverter fault current at PCC starts decreasing as shown in Fig. 5(c). The PV inverter current at PCC becomes zero within 1.8 ms upon the response of slope detector. It is also noticed from Fig. 5(c) that the inverter current does not exceed its maximum rated value i.e. 1 p.u. during fault condition.

C. DIFFERENT FAULTS AT DIFFERENT TIME INSTANTS

Fault studies are performed by applying different types of faults at different time instants and it is confirmed that the controller responds in the expected manner regardless of any type of fault at any time instant. Due to lack of space, only one of the above studies is presented below.

Fig. 6(a) depicts that the magnitude of inverter output current at PCC increases from 1 p.u. to 1.45 p.u. during line-to-line ground fault at $t = 4.5$ second. It is seen from Fig. 6(a) that the fault occurs near the peak instant of an inverter current of phase B and one of the phase currents tends to exceed 1 p.u.

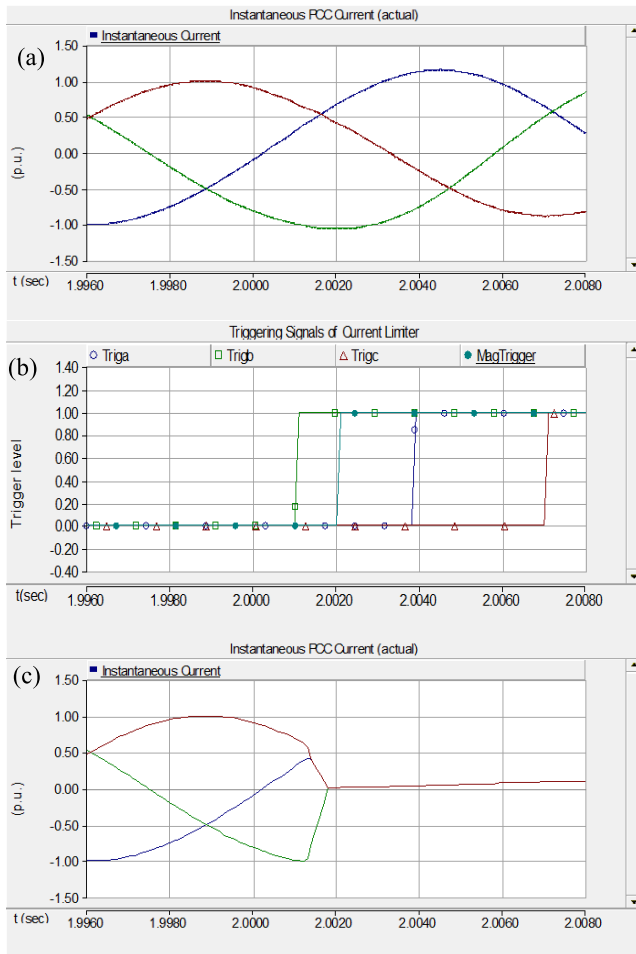


FIGURE 5. (a) Inverter fault current at PCC during SLG fault at $t = 2$ seconds. (b) Triggering signals. (c) Inverter fault current with proposed fault controller.

after the fault occurs. As soon as the magnitude of phase B current ($|I|_{max}$) exceeds its allowable limit, 'MagTrigger' signal gets high within 0.7 ms from the initiation of fault in the grid. Inverter fault current at PCC starts decreasing immediately upon detection of fault as shown in Fig. 6(c). Finally, the inverter current at PCC reaches zero within 1.3 ms based on the response of magnitude detector. Hence, if the fault occurs near the peak instant, the response of magnitude detector may be faster than the slope detector and the inverter current is prevented from exceeding its maximum rated value. Therefore, there is no apprehension of any adverse short circuit current contribution from the PV inverter.

D. LOAD SWITCHING

The performance of the controller is tested for two large load switching scenarios. In one study the large adjacent feeder load of 60 MVA at 0.9 pf is relocated to the feeder end next to the solar farm PCC, and switched on. In the second study, a 25 MVA induction motor load is switched at BUS 1 (Fig. 10).

Figs. 7 and 8 depict the inverter output and fault current detector signals for switching of 60 MVA static load

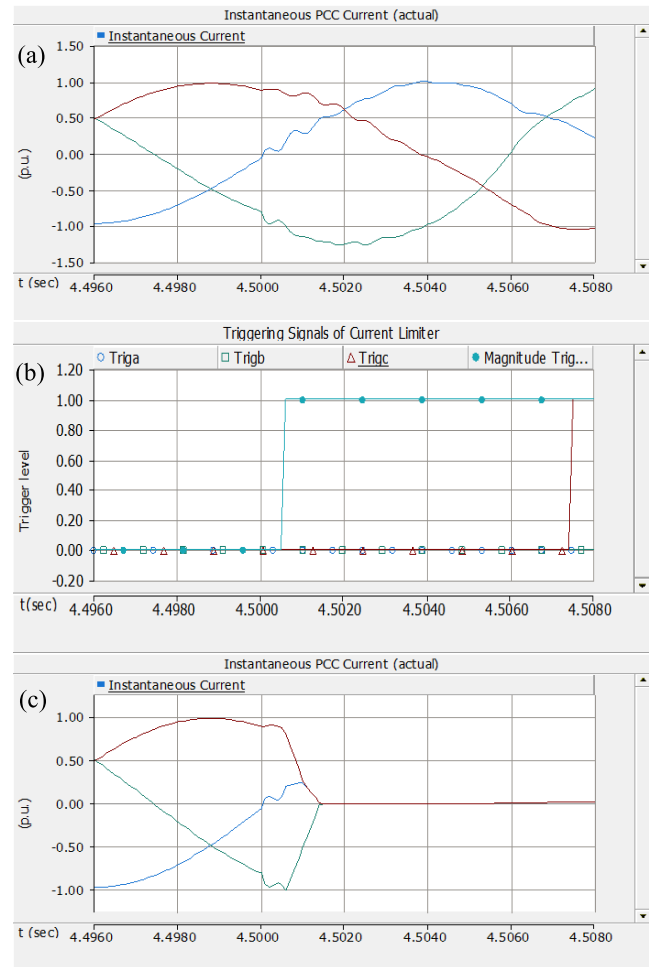


FIGURE 6. (a) Inverter fault current at PCC during LLG fault at $t = 4.5$ seconds. (b) Triggering signals. (c) Inverter fault current with proposed fault controller.

and 25 MVA induction motor, respectively. The inverter terminal voltage is depicted in Fig. 7(a) and 8(a). The instantaneous output currents of the inverter are demonstrated in Fig. 7(b) and 8(b), triggering signals generated by the slope detectors and magnitude detector are illustrated in Fig. 7(c) and 8(c), and the triggering signals (PVIso) generated by fault current detector are shown in Fig. 7(d) and 8(d), respectively. It is observed that the controller does not respond to both these load switching events. The steep rate of change in current at the instant of the load switching exceeds the limit for the slope detector and generates a tripping signal. However, the rate of change of voltage is within the predetermined limit and therefore the voltage detector output is zero. A logical ANDING of both these signals results in a zero output. A false tripping signal is thus prevented.

The controller is also tested for its performance during the reclosure operation of a relay. Fig. 9 illustrates the inverter output and fault current controller response for fast reclosure operation of the relay. The inverter terminal voltage is depicted in Fig. 9(a), the inverter output current is demonstrated in Fig. 9(b), the output of slope detectors and

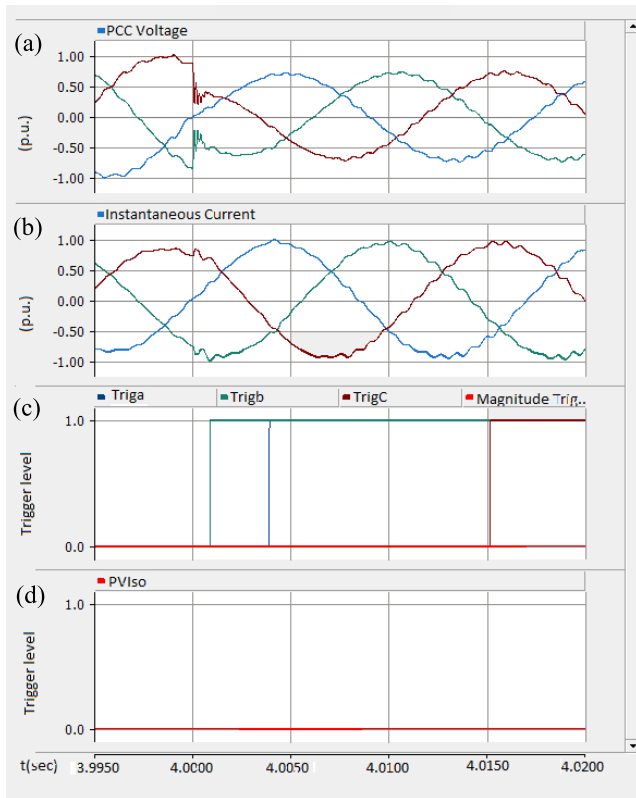


FIGURE 7. Response of proposed controller for switching of 60 MVA static load at feeder end. (a) PCC voltage. (b) Instantaneous inverter current. (c) Triggering signals from fault detection module. (d) PV isolation signal.

magnitude detectors are illustrated in Fig. 9(c), and the triggering signal generated by the fault current controller (PV Iso) is shown in Fig. 9(d). It is seen that, during reclosure operation the slope detector issues a tripping signal. But similar to load switching, the rate of change of voltage is less than the reference value and thus the overall fault detector does not generate any tripping signal. This demonstrates that the short circuit current controller can successfully discriminate between a fault and other transient high current events.

The above studies illustrate that in regions where the grid codes do not require LVRT, and require DG inverters to shut down following a fault, the proposed predictive technique shuts off the PV inverter rapidly without allowing the short circuit current to exceed the rated current of the inverter.

IV. GRID VOLTAGE SUPPORT DURING FAULT

The application of the proposed short circuit current detector for providing rapid reactive power support to stabilize a critical induction motor is shown in this section. This application is especially relevant in jurisdictions where the grid codes require LVRT capability or a grid support function from DG inverters during faults.

In this application, the proposed fault current controller is integrated with the PV system to very rapidly identify the occurrence of a grid fault situation which may cause the inverter current to exceed its rated value. In this

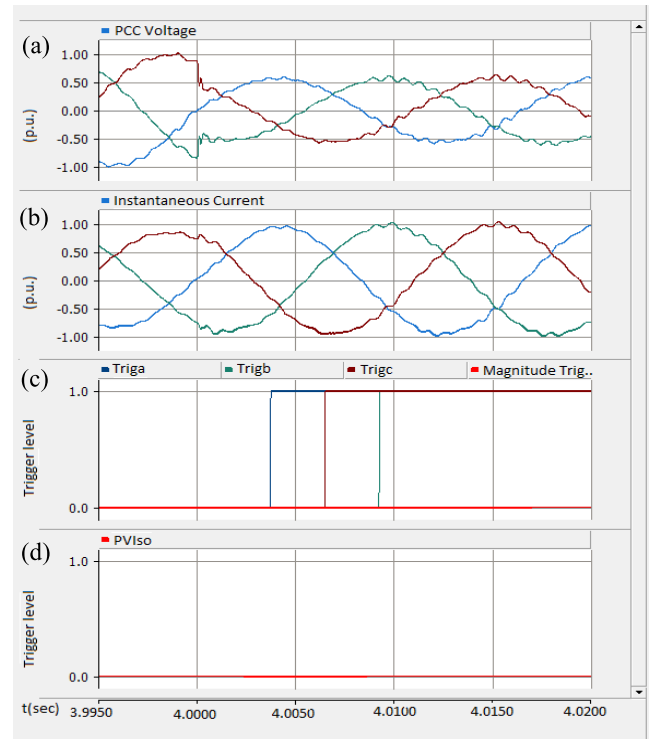


FIGURE 8. Response of proposed controller for switching of 25 MVA induction motor load at feeder end. (a) PCC voltage. (b) Instantaneous inverter current. (c) Triggering signals from fault detection module. (d) PV isolation signal.

case the inverter is not shut down but immediately and autonomously transformed into a dynamic reactive power compensator STATCOM (termed PV-STATCOM) to provide voltage support for stabilizing a critical induction motor (IM) load.

The study system is depicted in Fig. 10, which is a modified version of Fig. 1. A 400 hp (300kW) squirrel cage IM is considered to be the critical IM load connected at the end of the feeder. The IM parameters are obtained from the manufacturer’s datasheet of American Motors [37]. The obtained parameters are converted to fit into the EMTDC/PSCAD library model [38] by using the conversion expressions given in [39]. As the IM is rated for lower voltage, a step down transformer (not shown in the one line diagram) is used to match the IM voltage ratings. The PV solar farm is connected at an intermediate location in the feeder, away from the induction motor.

The PV-STATCOM controller is described in [27] and [28]. Due to space reasons the detailed description of the PV-STATCOM controller is not provided here, only its application in stabilizing the critical induction motor is presented. A three phase to ground fault for 9 cycles is initiated at the motor terminals in this case study.

A. CASE 1: CONVENTIONAL PV SYSTEM DISCONNECTED DURING FAULT

Fig. 11 illustrates the IM response for a LLLG fault at motor terminal. The voltage at the IM terminal is illustrated in

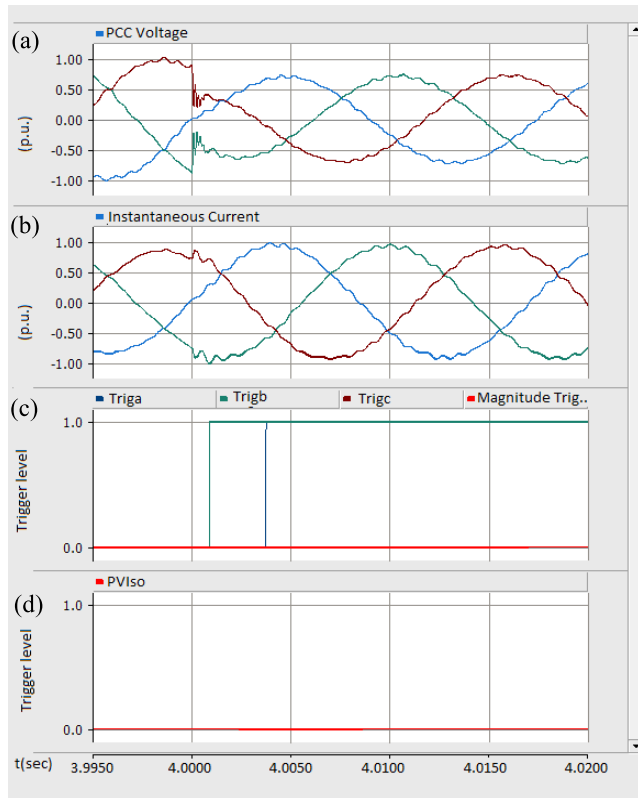


FIGURE 9. Response of proposed controller for fast reclosure operation of relay. (a) PCC voltage. (b) Instantaneous inverter current. (c) Triggering signals from fault detection module. (d) PV isolation signal.

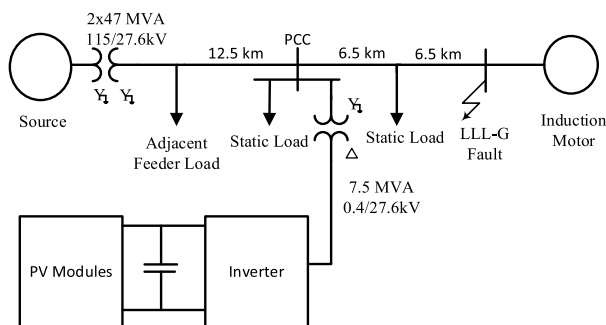


FIGURE 10. Study System for PV solar farm operation as STATCOM for stabilizing critical induction motor load.

Fig. 11(a), IM speed is shown in Fig. 11(b), DC power and real and reactive power generation by the PV solar farm are demonstrated in Fig. 11(c), the real and reactive power drawn by the IM are presented in Fig. 11(d), and DC link voltage is depicted in Fig. 11(e). The PV solar farm is considered to be disconnected during the fault and not provide any grid support.

During the fault, the voltage at the IM terminal becomes considerably low as illustrated in Fig. 11(a). Therefore, the IM speed decreases as portrayed in Fig. 11 (b). After the fault is cleared at $t = 5.15$ seconds, the voltage at the IM terminal recovers but the IM speed becomes unstable. This leads to the stalling of this critical induction motor.

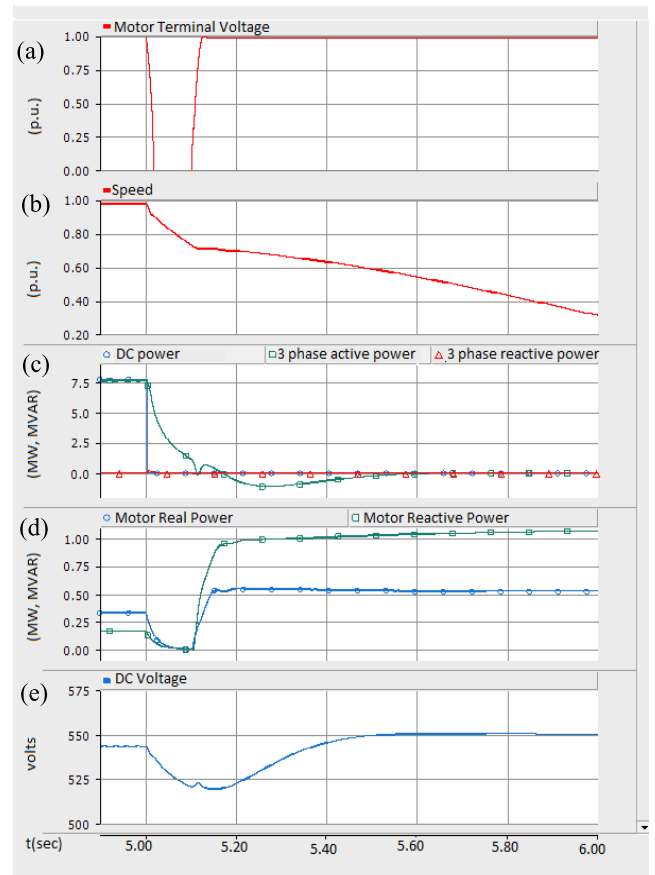


FIGURE 11. Behavior of induction motor load after grid fault. (a) Motor terminal voltage. (b) Motor speed. (c) DC power, three-phase AC real power, and three-phase AC reactive power of PV solar system. (d) Real and reactive power of motor. (e) PV inverter DC link voltage.

B. CASE 2: PV SYSTEM OPERATION AS PV-STATCOM

Fig. 12 illustrates the IM response when the proposed short circuit current detector rapidly detects the fault and transforms the PV solar farm into a PV-STATCOM in PCC Voltage control mode of operation. The triggering signal generated by the fault detector (PViso) is depicted in Fig. 12(a), voltage at IM terminal is illustrated in Fig. 12(b), IM speed is shown in Fig. 12(c), the DC power and the real and reactive power from the PV solar farm are demonstrated in Fig. 12(d), real and reactive power consumed by the IM is presented in Fig. 12(e) and PV system DC link voltage is depicted in Fig. 12(f). Since the PV solar farm transforms into a STATCOM (PV-STATCOM), the DC power generated by the PV modules reduces immediately to zero and the active power output of the PV inverter also gradually decreases to zero. The PV-STATCOM immediately starts producing reactive power and provides voltage support to the grid thereby stabilizing the critical induction motor. The reactive power of the PV-STATCOM eventually goes to zero after some time (which is not shown in the figure). The solar farm can autonomously transform back from PV-STATCOM mode to normal PV solar power generation mode after the motor is

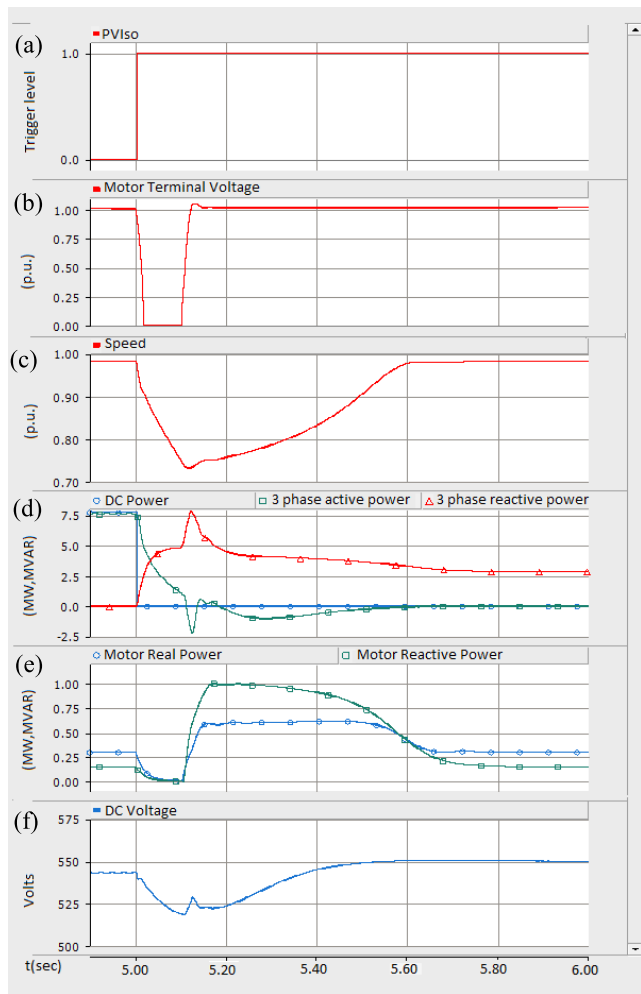


FIGURE 12. Behavior of induction motor with PV solar farm transformed into PV-STATCOM by the proposed short circuit current detector. (a) PV Isolation signal. (b) Motor terminal voltage. (c) Motor speed. (d) DC power, three-phase AC real power, and three-phase AC reactive power of PV solar system. (e) Real and reactive power of motor. (f) PV inverter DC link voltage.

stabilized (although not demonstrated in this paper due to space limitation).

V. DISCUSSION

It is clarified that this proposed technique is not a technique for detecting short circuit faults in the network. It is only intended to detect a fault condition in which the short circuit current from a PV inverter is likely to exceed the normal rated inverter current. If such a condition is detected the PV solar farm is either rapidly disconnected from the grid or autonomously transformed into a PV-STATCOM for providing reactive power support to the grid. The entire process of DG disconnection/transformation into PV-STATCOM from the instant of adverse short circuit current detection typically takes less than two millisecond. It is expected that implementation of this or similar short circuit current mitigation technique on PV inverters will prevent any adverse short circuit current contributions from solar farms, which was the

prime reason for the large-scale denial of their connectivity in Ontario. This will therefore create an opportunity to integrate more PV solar systems in Ontario and in similar jurisdictions. However, in regions where the grid codes allow PV solar farms to stay connected and provide grid support, the proposed technique can potentially be utilized to enable faster initiation of the LVRT function or rapidly transform the PV solar inverter into a STATCOM mode of operation for grid support.

This technique is developed assuming that the PV solar farm has only one inverter and is connected directly to the PCC without any intervening cables or lines. The principles of this technique can be adapted to large solar farms with multiple inverters, which may be located at a distance from the PCC. In this case coordination of multiple inverters, and delays in communication between measurements from the PCC to the individual inverters will need to be considered.

VI. CONCLUSION

In this paper, a novel fast short circuit current detection technique is proposed for PV inverter based DGs. The proposed short circuit current detector is based on the evaluation of the slope (d/dt) and magnitude of the PV inverter current. As soon as it detects a fault that is likely to cause the PV inverter short circuit current to exceed the rated current of the inverter, it can do either of the following depending upon the grid code being followed by the utility:

- i) disconnect the PV inverter from the grid so that it does not cause any adverse short circuit current injection into the grid, or
- ii) autonomously transform the PV inverter into a dynamic reactive power compensator STATCOM (termed PV-STATCOM) to provide grid voltage support. In this paper this voltage support is demonstrated for stabilizing a critical induction motor load.

The entire process of DG disconnection or transformation into a PV-STATCOM from the instant of fault detection typically takes about 1-2 millisecond. Through PSCAD/EMTDC simulation of a realistic distribution system this new controller is demonstrated to respond successfully regardless of the type of fault and the location of fault on the distribution system. The technique can successfully discriminate between faults and large load switching and relay initiated reclosure operations. This technique is general and can be applied on a PV solar system connected in any grid network.

A substantial number of connections of Photovoltaic (PV) solar Distributed Generators (DGs) in certain jurisdictions such as in Ontario, Canada, have been denied due to the potential of short circuit current contribution to the grid during faults. The application of this short circuit current technique has been demonstrated to shut down PV solar farms so as not to contribute any short circuit current into the grid, and thereby obviate the reason for which they were denied connectivity in jurisdictions as in Ontario which do not have an LVRT requirement at present. The objective of this technique is to facilitate PV solar farms in obtaining

permission to get connected in substations or feeders which have already reached their short circuit current limits without the apprehension of additional short circuit current contribution from these solar farms.

The disconnection of the inverter is needed in regions where LVRT is not a requirement as in Ontario. However, in regions where LVRT is a requirement, this technique is also beneficial for a faster initiation of grid support functions by the PV inverter. In this paper this fast fault detection technique is utilized to autonomously initiate a new control function of PV solar farm as a STATCOM (PV-STATCOM) for providing grid voltage support to stabilize a critical voltage sensitive Induction Motor load during a fault scenario.

APPENDIX

System Data [33], [34]:

Each set of 115kV/27.6 kV three phase transformer is configured with three single phase transformers having an impedance of 18.5%.

PV Module: 72.6 W, 67.9 V, 1.07 A, $V_{oc} = 90$ V, $I_{sc} = 1.19$ A.

No. of series modules = 8 and no. of parallel modules = 12905.

PI-1: $k_p = 1$, $T_i = 0.01$; PI-2: $k_p = 2$, $T_i = 0.0015$; PI-3: $k_p = 10$, $T_i = 0.015$,

PI-4: $k_p = 0$, $T_i = 0.005$

The LPF filter parameters for the d - q components are $G = 1.0433$ and $\tau = 0.1$ sec. The filter parameter for I_{o_a} , I_{o_b} and I_{o_c} feedback controller is $G = 1.5$ and $\tau = 0.003$ sec.

The reference value for rate limiter is 10038 [1/s], reference value for rate of change of voltage detector is 200 [1/s], and the R-S flip Flop delay time is 0.1 μ s.

REFERENCES

- [1] F. Katiraei, C. Sun, and B. Enayati, "No inverter left behind: Protection, controls, and testing for high penetrations of PV inverters on distribution systems," *IEEE Power Energy Mag.*, vol. 13, no. 2, pp. 43–49, Mar./Apr. 2015.
- [2] N. Nimpitiwan, G. T. Heydt, R. Ayyanar, and S. Suryanarayanan, "Fault current contribution from synchronous machine and inverter based distributed generators," *IEEE Trans. Power Del.*, vol. 22, no. 1, pp. 634–641, Jan. 2007.
- [3] M. E. Baran and I. El-Markaby, "Fault analysis on distribution feeders with distributed generators," *IEEE Trans. Power Syst.*, vol. 20, no. 4, pp. 1757–1764, Nov. 2005.
- [4] S. M. Brahma and A. A. Girgis, "Development of adaptive protection scheme for distribution systems with high penetration of distributed generation," *IEEE Trans. Power Del.*, vol. 19, no. 1, pp. 56–63, Jan. 2004.
- [5] W. Johnston and F. Katiraei, "Impact and sensitivity studies of PV inverters contribution to faults based on generic PV inverter models, Ontario Grid Connection Study," Canadian Solar Ind. Association (CanSIA), Tech. Rep., May 2012, p. 143.
- [6] R. J. Bravo, R. Yinger, and S. Robles, "Three phase solar photovoltaic inverter testing," in *Proc. IEEE Power Energy Soc. General Meeting*, Jul. 2013, pp. 1–5.
- [7] N. Jenkins, R. Allan, P. Crossley, D. Kirschen, and G. Strbac, *Embedded Generation*. London, U.K.: Institution Eng. Technol., 2000.
- [8] H. Hooshyar and M. E. Baran, "Fault analysis on distribution feeders with high penetration of PV systems," *IEEE Trans. Power Syst.*, vol. 28, no. 3, pp. 2890–2896, Aug. 2013.
- [9] "Distributed generation technical interconnection requirements; interconnection at voltages 50 kV and below, revision 2," doc. DT-10-015, Hydro One, Hydro One Networks Inc, Toronto, ON, Canada, Jun. 2011.
- [10] "BC hydro distributed generation. Technical interconnection requirements. 100 kW and below, revision 1," doc. DGTIR-100, Oct. 2014.
- [11] *General Use of Power Supplies*, Canadian Standards Association (CSA) Standard C22.2 107.1-01, 2011.
- [12] "E.ON netz grid code—High and extra high voltage, E.ON netz GmbH. Bayreuth, Germany." [Online]. Available: <http://www.eonnetz.com/Ressources/downloads/enenarhseng1.pdf> and [Online]. Available: http://www.nerc.com/docs/pc/ivgtf/German_EON_Grid_Code.pdf
- [13] (Mar. 8, 2013). "ENTSO-E network code for requirements for grid connection applicable to all generators." [Online]. Available: http://networkcodes.entsoe.eu/wp-content/uploads/2013/08/130308_Final_Version_NC_RfG1.pdf
- [14] "Recommendations for updating the technical requirements for inverters in distributed energy resources," Smart Inverter Working Group Recommendations, Sacramento, CA, USA, Jan. 2014.
- [15] Q. Wang, N. Zhou, and L. Ye, "Fault analysis for distribution networks with current-controlled three-phase inverter-interfaced distributed generators," *IEEE Trans. Power Del.*, vol. 30, no. 3, pp. 1532–1542, Jun. 2015.
- [16] P. Nuutinen, P. Peltoniemi, and P. Silventoinen, "Short-circuit protection in a converter-fed low-voltage distribution network," *IEEE Trans. Power Electron.*, vol. 28, no. 4, pp. 1587–1597, Apr. 2013.
- [17] M. Sumner, A. Abusorrah, D. Thomas, and P. Zanchetta, "Real time parameter estimation for power quality control and intelligent protection of grid-connected power electronic converters," *IEEE Trans. Smart Grid*, vol. 5, no. 4, pp. 1602–1607, Jul. 2014.
- [18] X. Pei and Y. Kang, "Short-circuit fault protection strategy for high-power three-phase three-wire inverter," *IEEE Trans. Ind. Informat.*, vol. 8, no. 3, pp. 545–553, Aug. 2012.
- [19] X. Liu, A. Thirumalai, and G. G. Karady, "Design and development of an ultra fast pilot protection," in *Proc. IEEE/PES Power Syst. Conf. Expo.*, Mar. 2011, pp. 1–7.
- [20] T. Ghanbari and E. Farjah, "Development of an efficient solid-state fault current limiter for microgrid," *IEEE Trans. Power Del.*, vol. 27, no. 4, pp. 1829–1834, Oct. 2012.
- [21] A. R. Fereidouni, B. Vahidi, and T. H. Mehr, "The impact of solid state fault current limiter on power network with wind-turbine power generation," *IEEE Trans. Smart Grid*, vol. 4, no. 2, pp. 1188–1196, Jun. 2013.
- [22] A. Abramovitz and K. M. Smedley, "Survey of solid-state fault current limiters," *IEEE Trans. Power Electron.*, vol. 27, no. 6, pp. 2770–2782, Jun. 2012.
- [23] A. Y. Wu and Y. Yin, "Fault-current limiter applications in medium- and high-voltage power distribution systems," *IEEE Trans. Ind. Appl.*, vol. 34, no. 1, pp. 236–242, Jan./Feb. 1998.
- [24] M. Ohrstrom and L. Soder, "Fast protection of strong power systems with fault current limiters and PLL-aided fault detection," *IEEE Trans. Power Del.*, vol. 26, no. 3, pp. 1538–1544, Jul. 2011.
- [25] Fault detection and short circuit current management technique for inverter based distributed generators (DG), by R. K. Varma and S. A. Rahman. (2015, Apr. 28). U.S. Patent 9 019 673.
- [26] R. K. Varma, V. Khadkikar, and R. Seethapathy, "Nighttime application of PV solar farm as STATCOM to regulate grid voltage," *IEEE Trans. Energy Convers.*, vol. 24, no. 4, pp. 983–985, Dec. 2009.
- [27] R. K. Varma, S. A. Rahman, A. C. Mahendra, R. Seethapathy, and T. Vanderheide, "Novel nighttime application of PV solar farms as STATCOM (PV-STATCOM)," in *Proc. IEEE PES General Meeting*, Jul. 2012, pp. 1–8.
- [28] R. K. Varma, S. A. Rahman, and T. Vanderheide, "New control of PV solar farm as STATCOM (PV-STATCOM) for increasing grid power transmission limits during night and day," *IEEE Trans. Power Del.*, vol. 30, no. 2, pp. 755–763, Apr. 2015.
- [29] R. K. Varma, "Multivariable modulator controller for power generation facility," Canada Patent PCT/CA2014/051 174, Dec. 6, 2014.
- [30] O. V. Thorsen and M. Dalva, "A survey of faults on induction motors in offshore oil industry, petrochemical industry, gas terminals, and oil refineries," *IEEE Trans. Ind. Appl.*, vol. 31, no. 5, pp. 1186–1196, Sep./Oct. 1995.
- [31] "The cost of power disturbances to industrial & digital companies," Electr. Power Res. Inst., White Paper, 2001, accessed on Aug. 23, 2012. [Online]. Available: <http://www.onpower.com/pdf/EPRICostOfPowerProblems.pdf>
- [32] R. K. Varma, S. A. Rahman, V. Sharma, and T. Vanderheide, "Novel control of a PV solar system as STATCOM (PV-STATCOM) for preventing instability of induction motor load," in *Proc. 25th IEEE Can. Conf. Elect. Comput. Eng. (CCECE)*, Apr./May 2012, pp. 1–5.

- [33] D. Turcotte and F. Katiraei, "Fault contribution of grid-connected inverters," in *Proc. IEEE Elect. Power Conf.*, Oct. 2009, pp. 1–5.
- [34] *Energy Wire and Cable for Power Generation, Transmission and Distribution, BICC Brand Product Catalogue*, General Cable, Highland Heights, KY, USA, Nov. 2011.
- [35] S. A. Rahman, R. K. Varma, and T. Vanderheide, "Generalised model of a photovoltaic panel," *IET Renew. Power Generat.*, vol. 8, no. 3, pp. 217–229, 2014.
- [36] G. Ortiz, D. Bortis, J. Biela, and J. W. Kolar, "Optimal design of a 3.5-kV/11-kW DC–DC converter for charging capacitor banks of power modulators," *IEEE Trans. Plasma Sci.*, vol. 38, no. 10, pp. 2565–2573, Oct. 2010.
- [37] J. Pedra, "On the determination of induction motor parameters from manufacturer data for electromagnetic transient programs," *IEEE Trans. Power Syst.*, vol. 23, no. 4, pp. 1709–1718, Nov. 2008.
- [38] *EMTDC/PSCAD User Manual*, HVDC Res. Center, MB, Canada, 2003. Also provide the city name.
- [39] J. Pedra, I. Candela, and L. Sainz, "Modelling of squirrel-cage induction motors for electromagnetic transient programs," *IET Electr. Power Appl.*, vol. 3, no. 2, pp. 111–122, 2009.



VISHWAJITSINH ATODARIA (S'14) received the B.E. degree in electronics engineering from Birla Vishwakarma Mahavidyalaya, Anand, India, in 2013, and the M.E.Sc. degree in power systems engineering from the University of Western Ontario, London, ON, Canada, in 2015.

He is presently a University Research Associate with Bluewater Power Distribution Corporation, Sarnia, ON, Canada. His research interests include grid integration of photovoltaic solar plants, and implementation of FACTS devices and their coordination.

Mr. Atodaria was a recipient of the Industrial Postgraduate Scholarship from the Natural Sciences and Engineering Research Council of Canada.



RAJIV K. VARMA (M'90–SM'09) received the B.Tech. and Ph.D. degrees in electrical engineering from IIT Kanpur, Kanpur, India, in 1980 and 1988, respectively.

He is currently a Professor with the University of Western Ontario, London, ON, Canada. He was the Hydro One Chair in power systems engineering with the University of Western Ontario from 2012 to 2015. He was a Faculty Member with the Electrical Engineering Department, IIT Kanpur,

from 1989 to 2001. He has coauthored a book entitled *Thyristor Based Facts Controllers* (IEEE Press/Wiley, 2002). His research interests include FACTS, power systems stability, and grid integration of wind and photovoltaic solar power systems.

Prof. Varma is active on a number of IEEE working groups. He has co-delivered several tutorials on SVC sponsored by the IEEE Substations Committee. He has been serving as the Chair of the IEEE Working Group on HVDC and FACTS Bibliography since 2004. He has been the Secretary of the IEEE HVDC and FACTS Subcommittee since 2015.



SIBIN MOHAN (M'04) received the B.Tech. degree in electrical and electronics engineering from Mahatma Gandhi University, Kottayam, India, in 2011, the M.Tech. degree in electrical engineering with a specialization in power electronics and power systems from IIT Bombay, Mumbai, India, in 2014, and is currently working toward the Ph.D. degree with the University of Western Ontario, London, Canada.

He is a Research Associate with Bluewater Power, Sarnia, ON, Canada. His research interest include smart inverters, distributed generation, FACTS, power system stability, and power system quality.

Mr. Mohan has been the Secretary of the IEEE Working Group on HVDC and FACTS Bibliography since 2015. He is a recipient of Industrial Postgraduate Scholarship from Natural Sciences and Engineering Research Council of Canada.



SHAH ARIFUR RAHMAN (S'09–M'12) received the Ph.D. degree from the University of Western Ontario, London, ON, Canada, in 2012.

He is currently a Post-Doctoral Fellow with the University of Western Ontario, London, ON, Canada, and performing research activities with Bluewater Power, Sarnia, ON, Canada. His research interests include grid integration of inverter based distributed generation (DG) sources, such as photovoltaic solar plants, wind farms, energy storage, impact analysis of harmonics and overvoltages on power systems, and implementation of FACTS capability in inverter based DGs and their coordination.

Dr. Rahman has been a Member of the IEEE Working Group on HVDC and FACTS Bibliography and Records since 2010. He served as a Secretary from 2012 to 2014.



TIM VANDERHEIDE is currently the Chief Operating Officer with Bluewater Power Renewable Energy Inc., Sarnia, ON, Canada, and Electek Power Services Inc., Sarnia, ON, Canada. He is also the Vice President of Strategic Planning with Bluewater Power Distribution Corporation, Sarnia, ON.